E-cadherin phosphorylation occurs during its biosynthesis to promote its cell surface stability and adhesion

Abbye E. McEwen[a,b,*], Meghan T. Maher[a,b,*], Rigen Mo[a,c], and Cara J. Gottardi[a]
[a]Department of Medicine and [b]Driskill Graduate Training Program in Life Sciences, Northwestern University Feinberg School of Medicine, Chicago, IL 60611; [c]Molecular Oncology Group, Kadmon Research Institute, New York, NY 10016

ABSTRACT **E-cadherin is highly phosphorylated within its β-catenin–binding region, and this phosphorylation increases its affinity for β-catenin in vitro. However, the identification of key serines responsible for most cadherin phosphorylation and the adhesive consequences of modification at such serines have remained unknown. In this study, we show that as few as three serines in the β-catenin–binding domain of E-cadherin are responsible for most radioactive phosphate incorporation. These serines are required for binding to β-catenin and the mutual stability of both E-cadherin and β-catenin. Cells expressing a phosphodeficient (3S>A) E-cadherin exhibit minimal cell–cell adhesion due to enhanced endocytosis and degradation through a lysosomal compartment. Conversely, negative charge substitution at these serines (3S>D) antagonizes cadherin endocytosis and restores wild-type levels of adhesion. The cadherin kinase is membrane proximal and modifies the cadherin before it reaches the cell surface. Together these data suggest that E-cadherin phosphorylation is largely constitutive and integral to cadherin–catenin complex formation, surface stability, and function.**

Monitoring Editor
Alpha Yap
University of Queensland

Received: Feb 12, 2014
Revised: Jun 12, 2014
Accepted: Jun 16, 2014

INTRODUCTION

Multicellular organisms require cadherin/catenin-based intercellular adhesion for normal cellular differentiation, tissue architecture, and tissue integrity. Cell–cell adhesion is mediated by a protein complex that comprises a transmembrane cadherin, which mediates Ca^{2+}-dependent homophilic recognition, and associated catenins, which link cadherins to the underlying cytoskeleton. Epithelial (E)-cadherin is the prototypic classical cadherin present on epithelia. The cytoplasmic domain of classical cadherins binds the dual-function adhesion/transcriptional regulatory proteins $p120^{ctn}$ and β-catenin (reviewed in McEwen *et al.*, 2012). $p120^{ctn}$ binds a membrane-proximal region of the cadherin tail and promotes cadherin stability at the cell surface by occluding an endocytosis signal (Kowalczyk and Nanes, 2012; Nanes *et al.*, 2012). β-Catenin binds the cadherin tail more distally and recruits the F-actin–binding protein α-catenin, coordinating cadherins with the cortical actin cytoskeleton (Maiden *et al.*, 2013). Numerous loss-of-function studies from both flies and vertebrates have demonstrated that each component in this complex is required for cell–cell adhesion and tissue morphogenesis (Peifer *et al.*, 1993; Larue *et al.*, 1994; Tepass *et al.*, 1996; Torres *et al.*, 1997; Vasioukhin *et al.*, 2001; Fukunaga *et al.*, 2005; Sarpal *et al.*, 2012); however, these studies provide limited insight into how adhesion is normally regulated.

Throughout tissue development, cells regulate their adhesiveness on the time scale of minutes (e.g., sea urchin epithelial–mesenchymal transition [EMT]; Wu *et al.*, 2007), which suggests the use of posttranscriptional mechanisms. Several models have been proposed to regulate adhesive strength and dynamics required for tissue morphogenesis: 1) regulation of cadherin cell surface delivery/stabilization (Le *et al.*, 1999), 2) phosphomodulation of β-catenin binding to cadherin (Lickert *et al.*, 2000) or α-catenin binding to β-catenin (Bullions *et al.*, 1997), 3) modulation of the association between α-catenin and the actin cytoskeleton (reviewed in Maiden *et al.*, 2013), 4) *cis* clustering of cadherins (Yap *et al.*, 1997), and 5) conformational regulation of the cadherin ectodomain (Petrova

This article was published online ahead of print in MBoC in Press (http://www.molbiolcell.org/cgi/doi/10.1091/mbc.E14-01-0690) on June 25, 2014.

*These authors contributed equally to this work.

Address correspondence to: Cara J. Gottardi (c-gottardi@northwestern.edu)

Abbreviations used: CK2, casein kinase 2; EMT, epithelial mesenchymal transition; GSK3, glycogen synthase kinase 3; IL2R, interleukin 2 receptor; Myr, myristoylation.

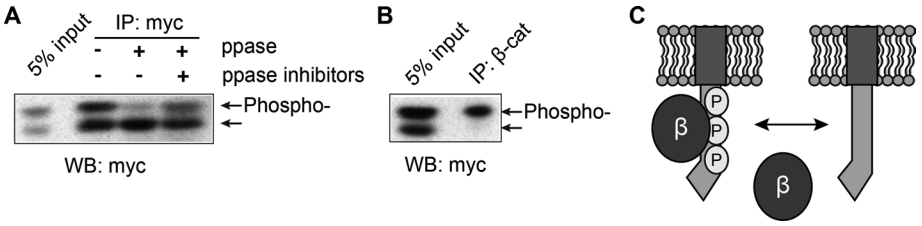

FIGURE 1: Endogenous β-catenin preferentially binds the phosphorylated form of the cadherin cytoplasmic domain in vivo. (A) Western blot (WB) of HEK293T cells transiently transfected with myc-tagged cadherin cytoplasmic domain (myc-cad-cyto) and immunoprecipitated (IP) with anti-myc antibody, followed by treatment with λ phosphatase ± phosphatase inhibitors. Arrows indicate slower-migrating (phosphorylated) and unphosphorylated cadherin. (B) Western blot of β-catenin immunoprecipitated from HEK293T cells transiently expressing myc-cad cyto. (C) Model shows that β-catenin preferentially interacts with phosphorylated cadherin cytodomain in cells.

et al., 2012). The cellular signals and modifications that affect these modes of regulation are just emerging (reviewed in Nelson, 2008; Niessen *et al.*, 2011).

It has been long appreciated that E-cadherin is a phosphoprotein (Stappert and Kemler, 1994). E-cadherin phosphorylation was first observed during mouse embryo compaction during the eight-cell stage (Sefton *et al.*, 1992), suggesting that this phosphorylation could positively affect cell–cell adhesion. These phosphorylations were later mapped to eight serine residues within a serine/threonine-rich 30–amino acid region that binds β-catenin and is conserved across all of the classical cadherins (Ozawa *et al.*, 1990; Stappert and Kemler, 1994). Mutagenesis of all eight serine residues to alanines generates a cadherin that cannot bind to β-catenin and fails to confer adhesive activity, which mimics a mutant E-cadherin lacking the entire β-catenin–binding domain (Stappert and Kemler, 1994), suggesting that these serines critically contribute to the E-cadherin/β-catenin–binding interface. Indeed, phosphorylation of E-cadherin in vitro by the general kinase CK2 or GSK-3β leads to a substantial (>800-fold) increase in the affinity of E-cadherin for β-catenin (Lickert *et al.*, 2000; Serres *et al.*, 2000; Choi *et al.*, 2006), which can be rationalized at the structural level (Huber *et al.*, 2001). However, the identification of key serines responsible for most cadherin phosphorylation and the in vivo consequences of modification at such serines have remained unknown. In this work, we show that as few as three serines in the β-catenin–binding domain of E-cadherin are responsible for most radioactive phosphate incorporation and that modification of these serines appears to be required for intercellular adhesion by stabilizing the cadherin at the cell surface.

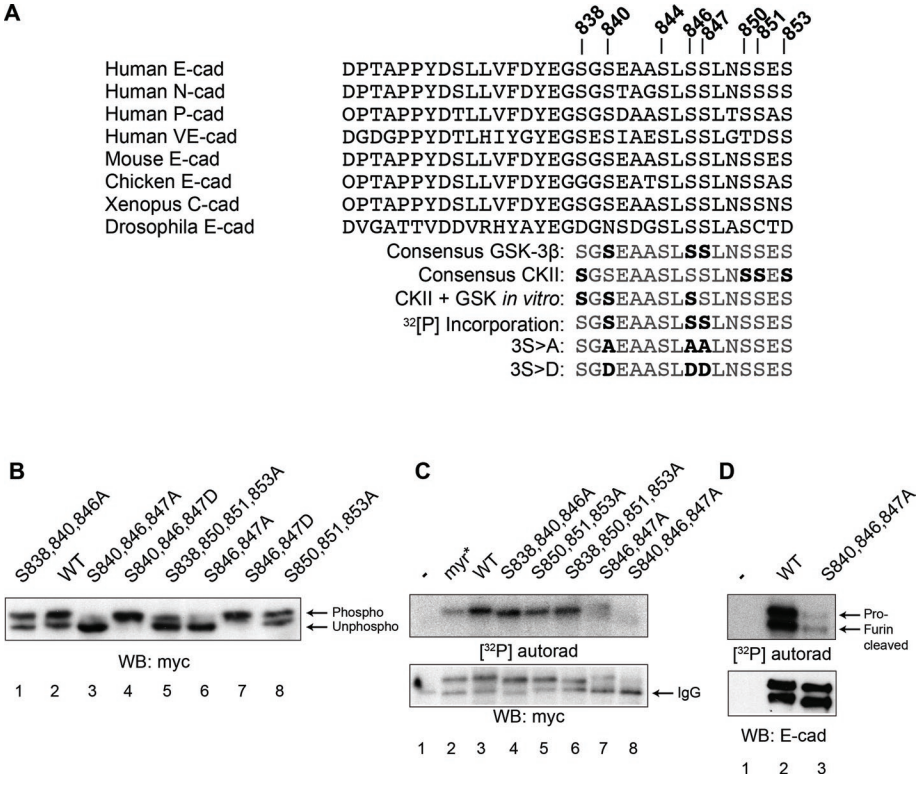

FIGURE 2: Serines 840, 846, and 847 are required for most radioactive orthophosphate labeling of E-cadherin. (A) Schematic of classical cadherin sequences across species reveals the conservation of serine resides in the β-catenin–binding region. GSK3 and CK2 consensus sites, as well as those visible in the crystal structure by Huber and Weis (2001), are shown below and in boldface. Serine-to-alanine (3S>A) or -aspartate (3S>D) mutant forms of the cadherin used in this study are also shown. (B) Western blot of HEK293T cells transiently transfected with E-cadherin tail and immunoblotted for myc. Arrows indicate phospho- and unphospho-E-cadherin forms. (C) Autoradiograph and Western blot of COS-7 cells transiently transfected with E-cadherin tail labeled with [32P]orthophosphate and immunoprecipitated with antibodies to the myc epitope. Nitrocellulose was first dried and exposed to film (top) and then immunoblotted with antibodies to myc (bottom). (D) Autoradiograph and Western blot of COS-7 cells transiently transfected with full-length E-cadherin labeled with [32P]orthophosphate and immunoprecipitated with antibodies to E-cadherin.

RESULTS

Cadherin phosphorylation regulates binding to β-catenin in vivo

To follow cadherin phosphorylation in vivo, we developed a nonradioactive mobility shift assay using the cytoplasmic domain of *Xenopus* C-cadherin, which runs as a doublet on SDS-polyacrylamide gels (Figure 1A, lane 1). Evidence that the slower-migrating form disappears upon treatment with λ-phosphatase suggests that this decreased mobility may be due to phosphorylation (Figure 1A, lanes 2 and 3). Indeed, only the slower-migrating form of the cadherin tail incorporates [32P]orthophosphate (Figure 2C, lane 3). To determine whether cadherin phosphorylation affects binding to β-catenin in cells, we immunoprecipitated β-catenin from cells transfected with the cadherin cytodomain and found that only the slower-migrating form of the cadherin associates with β-catenin (Figure 1B). These results indicate that β-catenin preferentially binds a phosphorylated cadherin under immunoprecipitation conditions (Figure 1C). This suggests that cadherin phosphorylation may be regulated to modulate β-catenin binding, which would be

relevant to both adhesive and nuclear signaling functions of β-catenin.

Identification of three serine residues responsible for steady-state E-cadherin phosphorylation

The β-catenin–binding domain of human E-cadherin contains eight serines that are highly conserved across classical cadherins from both vertebrate and invertebrate organisms (Figure 2A). Removing all eight serines abrogates most E-cadherin phosphorylation in vivo (Stappert and Kemler, 1994); however, identification of exactly which of these serines are most critical to cadherin phosphorylation remains unknown. To answer this question, we took a bioinformatics approach to guide our site-directed mutagenesis studies. Kinase prediction software (NetPhos2.0 and PhosphoSitePlus) revealed phosphorylation consensus sites for casein kinase II (CKII) and glycogen synthase kinase 3 (GSK3; Figure 2A, bottom alignment, in bold), two kinases capable of phosphorylating E-cadherin in vitro (Lickert *et al.*, 2000; Huber and Weis, 2001). A subset of these sites was also observed when recombinant E-cadherin cytodomain was in vitro phosphorylated with both CKII and GSK and then cocrystallized with the armadillo repeats of β-catenin (Huber and Weis, 2001). This combinatorial phosphorylation resulted in specific phosphoserine interactions with β-catenin and the binding of otherwise disordered flanking cadherin sequences (Huber and Weis, 2001), as well as an ~800-fold increase in affinity as measured by isothermal calorimetry (Choi *et al.*, 2006; Figure 2A, CKII + GSK3 in vitro). By making serine (S)-to-alanine (A) mutations in these putative CKII sites, GSK3β sites, or sites visible in the cocrystal structure, we find that only the GSK3 consensus S>A mutations abrogated the mobility shift (Figure 2B, lane 3) and incorporation of [^{32}P]orthophosphate into the E-cadherin tail (Figure 2C, lane 8). Evidence that aspartate (D) substitution of these same S residues fully restores the upward mobility shift seen in the wild-type (WT) cadherin (Figure 2B, lanes 4 and 7) suggests that the negative charges conferred by the aspartic acid side chain (CH_2COOH) mimic the phosphorylated ($–PO_4$) serines in the WT cadherin. Finally, S>A conversion of serines 840, 846, and 847 within a full-length E-cadherin protein almost completely blocks ^{32}P incorporation (Figure 2D, lane 3). Together these data show that as few as three serines within the eight-serine-containing β-catenin–binding domain are responsible for nearly all cadherin phosphorylation under steady-state conditions.

Serines 840, 846, and 847 are required for E-cadherin–based adhesion by promoting binding and stabilization of β-catenin

To address the contribution of serines 840, 846, and 847 and their charge status to β-catenin binding and cadherin function, we expressed WT, 3S>A, and 3S>D E-cadherins (Figure 2A) in the pan-cadherin–null cell line A431D, which is derived from human vulvar epidermoid carcinoma and often used for cadherin structure–function studies (Lewis *et al.*, 1997). Under steady-state conditions, we observed that the 3S>A cadherin accumulates less than either WT or 3S>D proteins (Figure 3A, input lanes). Because the cadherin tail is unstructured and unstable in the absence of β-catenin binding (Huber *et al.*, 2001), we reasoned that the 3S>A mutant fails to accumulate due to a reduced capacity to bind β-catenin. Both WT and 3S>D cadherins coimmunoprecipitate more β-catenin than the 3S>A cadherin mutant (Figure 3B). More important, the 3S>A E-cadherin stabilizes less β-catenin protein than WT and 3S>D E-cadherins (Figure 3B, left input lanes), suggesting that these serines are required for β-catenin binding *within cells* and not just under immunoprecipitation (IP) conditions that may not reflect binding differences under normal physiological concentrations of these proteins (Figure 3B, right IP lanes). Cadherins stabilize β-catenin at the protein level by binding to nascent β-catenin and preventing its continual degradation by the axin-destruction complex (Simcha *et al.*, 2001). Further confirming these findings, 3S>A E-cadherin fails to colocalize with β-catenin in both A431D (Figure 3D) and Madin–Darby canine kidney (MDCK; Figure 4C) cells and is unable to support strong intercellular adhesion using a neutral protease (dispase) mechanical disruption assay (Figure 3C). Moreover, 3S>A E-cadherin does not inhibit cell motility as well as WT and 3S>D E-cadherins, as assessed by a Boyden chamber–based chemotaxis assay (Supplemental Figure S1). Because aspartic acid substitution of serines 840, 846, and 847 generates a cadherin that appears structurally and functionally similar to WT E-cadherin but alanine substitution does not, it is likely that the WT cadherin is constitutively phosphorylated at these sites and that negative charges at these residues are critical for β-catenin binding and the mutual stabilization of β-catenin and E-cadherin.

Negative charge substitution of serines 840, 846, and 847 rescues E-cadherin surface levels and junctional organization

Previous data showed that the β-catenin–binding domain of E-cadherin is important for E-cadherin accumulation at the cell surface (Chen *et al.*, 1999). We sought to revisit this question in the context of our minimal E-cadherin mutants that block and mimic phosphorylation. Using immunofluorescence double-labeling analysis of E-cadherin with the pan–plasma membrane marker Na,K-ATPase, we show that the WT and the 3S>D cadherins localize to cell–cell contacts, whereas the 3S>A mutant does not (Figure 3E). However, the reduction in cell surface biotinylatable 3S>A E-cad relative to WT and 3S>D cadherins simply reflects their total protein levels (Figure 3A). Cells expressing 3S>A E-cadherin also show reduced capacity to promote tight junction (TJ) organization as assessed by ZO-1 staining, whereas the 3S>D phospho charge mimic rescues TJ formation to WT levels (Figure 3F), consistent with evidence that E-cadherin–based adhesion is required for tight junction barrier function (Gumbiner and Simons, 1987; Tunggal *et al.*, 2005). Taken together, these data suggest that phosphorylation at serines 840, 846, and 847 is required for the accumulation of E-cadherin at cell–cell contacts and the resulting intercellular adhesiveness and tight junction organization.

Serines 840, 846, and 847 are required for E-cadherin cell surface stability, and aspartate substitution limits endocytosis and targeting to lysosomes

Evidence that the 3S>A mutant fails to accumulate to the same extent as WT and 3S>D cadherins in A431D cells (Figure 3) suggests that the trafficking properties of E-cadherin may be impacted by phosphorylation. To address this, we sought to use MDCK cells, a nontransformed, spontaneously immortalized cell line that is typically used for trafficking studies (Dukes *et al.*, 2011). Distinct from the A431D cell system, which is pan-cadherin null and thus useful for determining the sole contribution of WT, 3S>A, and 3S>D cadherins to adhesive function and junction formation (Figure 3), MDCK cells express endogenous cadherins (Supplemental Figure S2). This allowed us to interrogate trafficking differences between our WT, 3S>A, and 3S>D E-cadherins in the context of well-formed cell–cell adhesions. Despite the differences between the A431D and MDCK cell systems, the 3S>A cadherin protein also accumulates less than either the WT or 3S>D proteins in MDCK cells (Figure 4A, left).

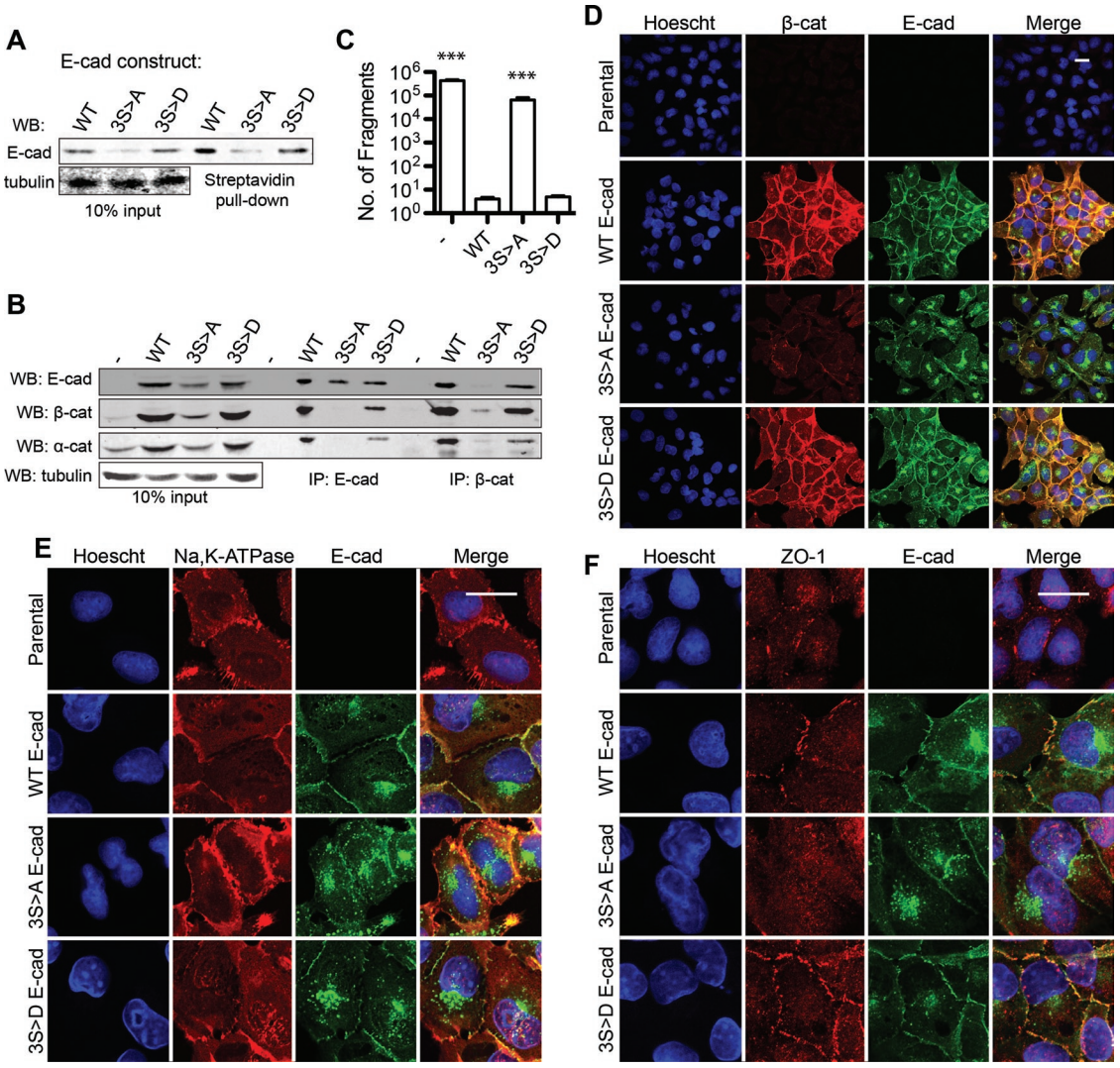

FIGURE 3: Fixed negative charges at serines 840, 846, and 847 promote surface localization of E-cadherin and binding to and stabilization of β-catenin. Analysis of pan-cadherin–null A431D cells reconstituted with full-length E-cadherin-Dendra2 (WT, 3S>A, or 3S<D). (A) Cell surface accumulation of E-cadherin constructs. Membrane proteins were labeled with biotin, enriched with streptavidin beads, and immunoblotted with antibodies as indicated. (B) Western blot of A431D reconstituted cell lines immunoprecipitated with anti-E-cadherin or anti–β-catenin. (C) Intercellular adhesion assay. Monolayers were released with dispase and subjected to shaking. Graph shows the number of fragments counted after shaking. Results are represented as the mean of six replicates. Error bars represent SEM. Asterisks represent statistically different from WT (***$p < 0.001$). Cells were fixed and stained for (D) β-catenin, (E) Na,K-ATPase, or (F) ZO-1 (red) and counterstained with E-cadherin (green). Bar, 25 μm.

These differences do not covary with mRNA levels (Supplemental Figure S3), suggesting that the 3S>A mutant is less stable at the protein level. In addition, upon treatment of cells with the lysosome inhibitor chloroquine (CQ), the 3S>A E-cadherin is present in amounts similar to WT and 3S>D E-cadherin (Figure 4A, right), suggesting that the 3S>A cadherin is being degraded to a greater extent by a lysosomal pathway as compared with WT or 3S>D. Consistent with these data, the 3S>A E-cadherin shows enhanced colocalization with the lysosome marker Lamp2 as compared with either WT or 3S>D cadherins (Figure 4B), which demonstrates that the 3S>A mutant exhibits enhanced targeting to lysosomes. WT, 3S>A, and 3S>D E-cadherins equally colocalize with the *cis*-Golgi marker GM130. Consistent with the enhanced localization of the 3S>A mutant to lysosomes, we found that the 3S>A E-cadherin mutant has a shorter half-life (~1 h) than WT and 3S>D (~2–5 h; Supplemental Figure S4). This reduced stability of 3S>A E-cadherin is at least in part due to its faster removal from the cell surface, as 3S>A E-cadherin labeled at the cell surface with biotin is degraded faster than either the WT or 3S>D biotinylated cadherins (Figure 4, E and F). Together these results indicate that serines 840, 846, and 847 are required for E-cadherin cell surface stability and that negative charge substitution at these residues limits cadherin degradation by lysosomes.

Negative charge substitution of serines 840, 846, and 847 limits E-cadherin endocytosis

Evidence that the 3S>A E-cadherin mutant exhibits less cell surface stability raises the possibility that it is endocytosed more rapidly than either the WT or the 3S>D E-cadherin. To study the effects of serines 840, 846, and 847 on cadherin endocytosis, we reengineered our

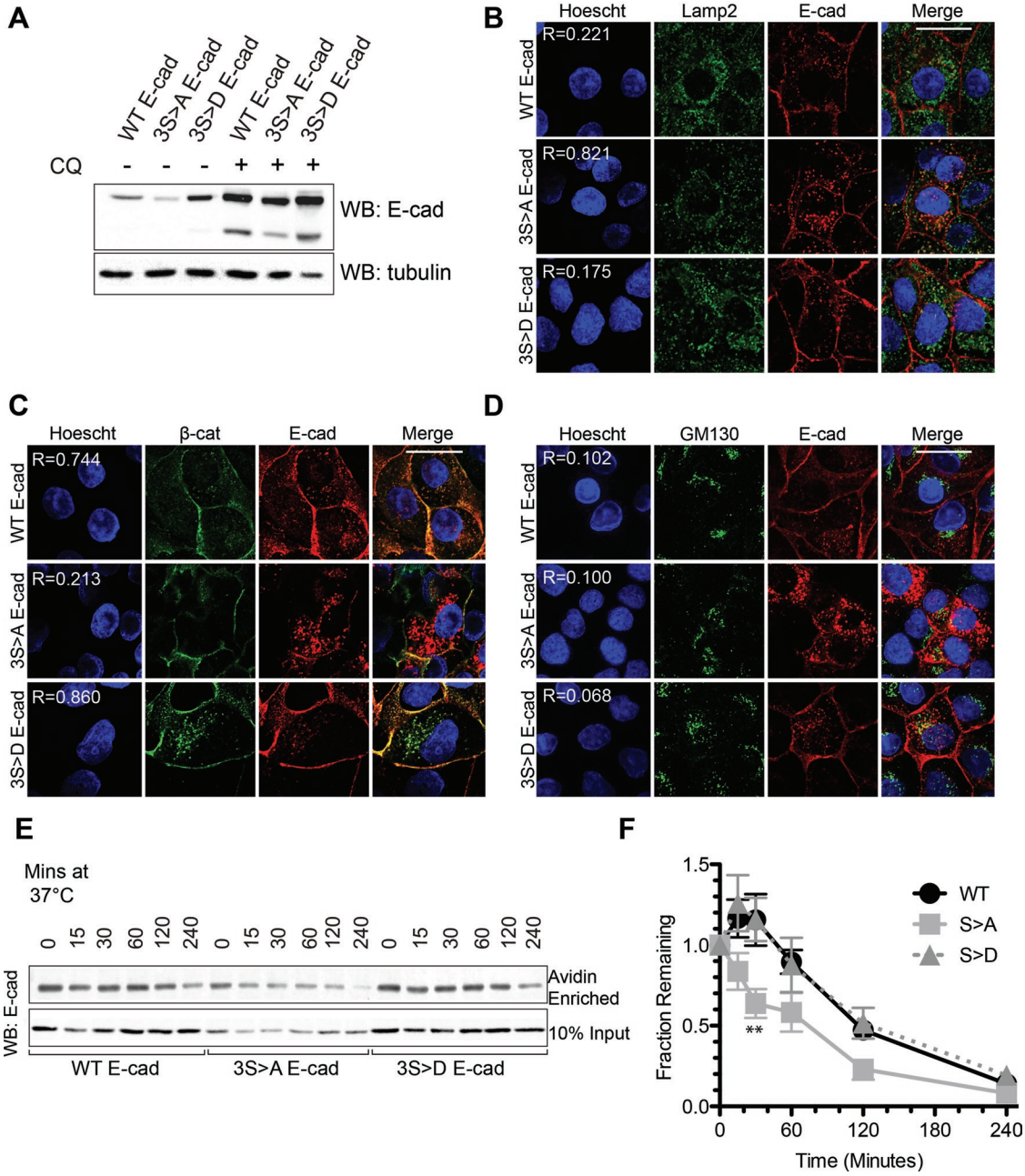

FIGURE 4: Fixed negative charges at serines 840, 846, and 847 promote E-cadherin stability. Analysis of MDCK cells stably transfected with full-length E-cadherin-Dendra2 (WT, 3S>A, or 3S>D). (A) Immunoblot for E-cadherin levels after 24 h of treatment with chloroquine diphosphate (CQ). Immunofluorescence double labeling of E-cadherin (red) and (B) the lysosomal marker lamp2, (C) β-catenin, or (D) the *cis*-Golgi maker GM130 (green). Bar, 25 μm. Colocalization measured by Pearson's coefficient (*R*). (E) Immunoblot and (F) quantification of surface E-cadherin degradation kinetics. Stability of surface E-cadherin was assessed using cell surface biotinylation, followed by incubation at 37°C for 15–240 min and enrichment with streptavidin beads. $N = 4$. Error bars represent SEM. Asterisks represent statistically different from WT (**$p < 0.01$).

3S>A and 3S>D mutants into fusion proteins containing the extracellular domain of the interleukin-2 receptor (IL2-R) fused to the cytoplasmic domain of E-cadherin. This construct design allowed us to determine the contribution of cadherin tail sequences to trafficking unimpeded by the homophilic cadherin ectodomain interactions (Xiao *et al.*, 2005). We observed that the 3S>A IL2-R-E-caderin mutant was endocytosed to a greater extent than either the WT or 3S>D IL2-R-E-cadherins (Figure 5, A and B) or the IL2-R alone (Supplemental Figure S5). Moreover, the WT and 3S>D E-cadherins showed membrane-proximal staining patterns, whereas the 3S>A showed a perinuclear pattern resembling lysosomal staining (Figure 5A). We confirmed these results using cell-surface biotinylation experiments in the context of full-length cadherin and found that over the course of 20 min, a greater fraction of the 3S>A E-cadherin is endocytosed than that of either the WT or 3S>D E-cadherin (Figure 5, C and D). Curiously, the 3S>D cadherin appears to be endocytosed

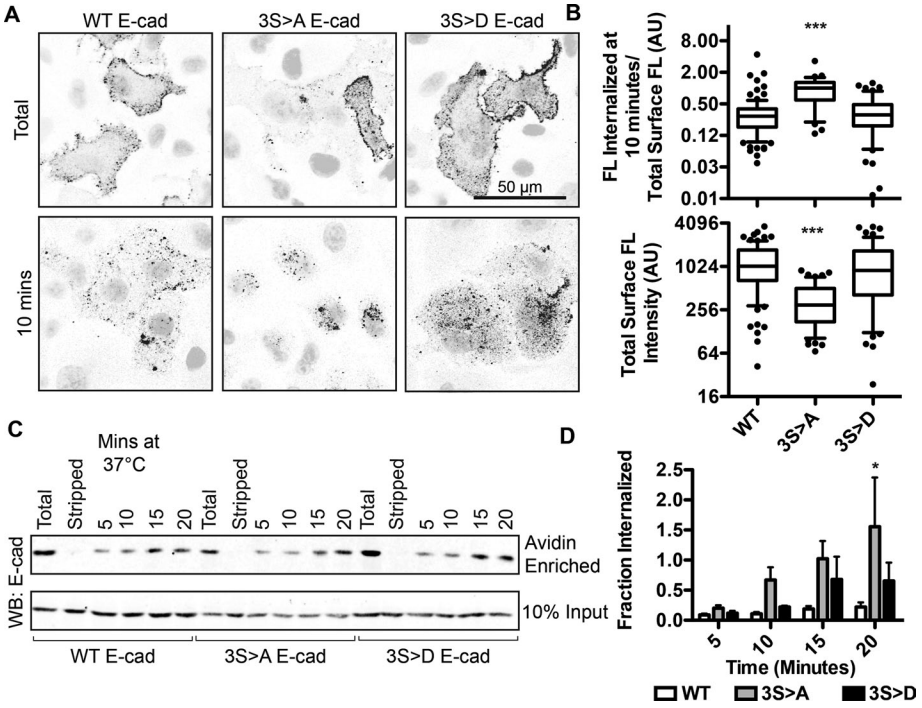

FIGURE 5: Serine-to-alanine substitution at 840, 846, and 847 promotes E-cadherin internalization. (A) Fluorescence-based endocytosis assay. MDCK cells stably transfected with an IL-2R-E-cadherin fusion (WT, 3S>A, or 3S>D) were labeled with anti–IL-2R, followed by a 10-min incubation at 37°C to induce endocytosis and an acid wash to remove remaining surface antibody. Cells were fixed and stained, and fluorescence intensity was quantified before and after endocytosis. (B) Graph representative of two independent experiments (number of cells counted, 37–98 cells/condition). Whiskers represent 10th to 90th percentile. (C) Immunoblot and (D) quantification of internalization kinetics of full-length E-cadherin MDCK cells stably transfected with E-cadherin-Dendra2 (WT, 3S>A, or 3S>D) labeled with biotin. Endocytosis was induced at 37°C, the remaining surface biotin was stripped, and internalized proteins were enriched with streptavidin beads. Error bars represent SEM of two or three independent experiments per construct. Asterisks represent statistically different from WT (*$p < 0.05$; ***$p < 0.001$).

faster than WT but slower than the 3S>A cadherin, suggesting that, in this functional assay, aspartate substitution at serines 840, 846, and 847 limits E-cadherin endocytosis but not as reliably as the WT cadherin. When internalization kinetics experiments were carried out over the course of 120 min, we observed that WT E-cadherin accumulated over time, in contrast to the 3S<A mutant, whose internalized signal peaked at 15 min and then began to disappear (Supplemental Figure S6), suggesting that the endocytosed pool of 3S<A E-cadherin is degraded more rapidly than WT. We also observed that the internalized signal for the 3S>D E-cadherin mutant decreased over time. Because the 3S>D mutant has degradation kinetics similar to that of WT E-cadherin (Supplemental Figure S4 and Figure 4F), this may suggest that the internalized pool of 3S>D E-cadherin is recycled back to the cell surface.

The cadherin kinase is membrane proximal and modifies the cadherin during its biosynthesis and trafficking to the cell surface

Whereas serines 840, 846, and 847 appear to be responsible for E-cadherin phosphorylation and adhesive function, the location and identity of the cadherin kinase are not known. Given that the cadherin is a membrane protein, we reasoned that the cadherin kinase would be membrane localized. To address this, we generated a myristoylated version of the E-cadherin cytodomain (Myr-E-cad), as well as a point mutant that lacks the critical glycine required for modification (Myr*-E-cad; Figure 6A). As expected, we found that the Myr-E-cadherin showed enhanced [^{32}P]orthophosphate incorporation compared with the Myr*-E-cadherin (Figure 2C, lanes 2 and 3). The myristoylated E-cadherin is targeted to membranes effectively (Figure 6B), showed a higher ratio of slower-migrating to faster-migrating species under steady-state conditions (Figure 6C), and is converted more rapidly to the phospho form under [^{35}S]methionine/cysteine pulse-chase conditions (Figure 6D). In addition, the uncleaved, proform of full-length E-cadherin incorporates radioactive phosphate at the same level of intensity as the processed form (Figure 2D). Because furin (or subtilisin-like convertase)–mediated cleavage of the prodomain occurs in the Golgi complex (Posthaus *et al.*, 1998), these data indicate that cadherin phosphorylation occurs before that cleavage event. Finally, although serines 840, 846, and 847 conform to GSK3 consensus sites and Wnt3a can transiently reduce cadherin function in *Drosophila* S2 cells (Wodarz *et al.*, 2006), inhibition of GSK3β by LiCl or Wnt3a fails to affect the kinetics of cadherin phosphorylation as assessed by the mobility shift of the cadherin tail (Supplemental Figure S7). Moreover, mouse embryo fibroblasts (MEFs) lacking both GSK3α and β do not lose expression of the slower-migrating phospho-cadherin form (Supplemental Figure S8). Taken together, these data indicate that the cadherin kinase acts early during cadherin biosynthesis and that the kinase responsible for the mobility shift does not appear to be GSK3.

DISCUSSION

It has been known for some time that the cytoplasmic tail of E-cadherin is robustly phosphorylated in the β-catenin–binding region and that this phosphorylation increases the affinity for β-catenin in vitro (Stappert and Kemler, 1994; Lickert *et al.*, 2000; Choi *et al.*, 2006). However, the function and regulation of E-cadherin phosphorylation in vivo have remained poorly defined. Taking advantage of the observation that cadherin cytodomain phosphorylation can be followed by a simple mobility shift in SDS–polyacrylamide gels, we show that natively phosphorylated cadherin associates with β-catenin substantially more than unphosphorylated cadherin, indicating that modulation of E-cadherin phosphorylation in cells can affect the cadherin/β-catenin binding interaction. Given that β-catenin, or the related plakoglobin protein, is required for cadherin-based cell–cell adhesion (Peifer *et al.*, 1993; Fukunaga *et al.*, 2005), regulation of cadherin phosphorylation is expected to affect cadherin/catenin adhesive functions robustly.

We show that three serines within the β-catenin–binding domain of E-cadherin are responsible for most radioactive phosphate incorporation and that these serines are required for binding to β-catenin and the mutual stability of both E-cadherin and β-catenin. Cells expressing a phosphodeficient (3S>A) E-cadherin show little intercellular adhesion due to enhanced endocytosis

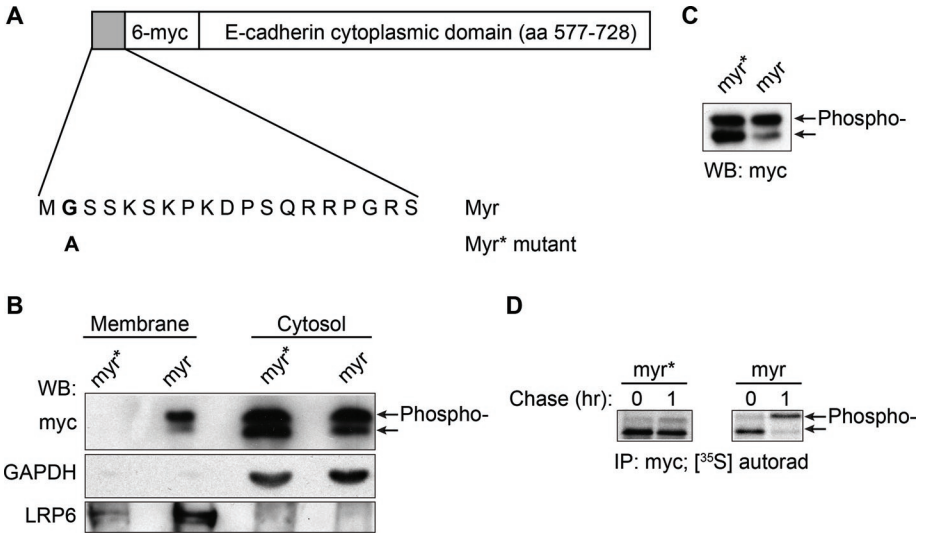

FIGURE 6: Membrane targeting of E-cadherin cytoplasmic domain enhances phosphorylation. (A) Schematic of wild-type myristoylation-tagged (myr) and myristoylation mutant (myr*)–tagged human E-cadherin cytoplasmic domain (E-cad cyto). (B) Immunoblot of membrane and cytosolic fractions from COS-7 cells transiently transfected with myr- or myr*-E-cad cyto. (C) Immunoblot from HEK293T cells expressing myr or myr* E-cad cyto. (D) Autoradiograph of COS-7 cells transiently expressing myr or myr* E-cad cyto were metabolically labeled with [^{35}S]methionine/cysteine for 20 min and then chased for 0 or 1 h. Cells were lysed and immunoprecipitated with antibodies to myc.

and degradation through a lysosomal compartment, whereas negative charge substitution at these serines (3S>D) antagonizes cadherin endocytosis and mimics wild-type E-cadherin trafficking and adhesion. Together with evidence that E-cadherin is phosphorylated before reaching the cell surface, these data suggest that cadherin phosphorylation is integral to cadherin–catenin complex formation, surface stability, and cell–cell adhesion.

Although our mobility shift assay for cadherin phosphorylation suggests that β-catenin cannot associate with an unphosphorylated cadherin (Figure 1), this assessment is inferred from dilute immunoprecipitation conditions rather than normal cellular concentrations of β-catenin and cadherins. Indeed, the β-catenin/unmodified cadherin binding affinity is found to be in the nanomolar range (Choi *et al.*, 2006), and the cellular concentration of β-catenin, estimated from undiluted *Xenopus* extracts as 25–153 nM and from mammalian cells as 390–1500 nM (Lee *et al.*, 2003; Tan *et al.*, 2012), suggests that β-catenin binding to an unphosphorylated cadherin is likely substantial within the cell. Nonetheless, evidence that β-catenin preferentially associates with a natively phosphorylated cadherin (Figure 1), where the β-catenin/in vitro phosphorylated cadherin–binding affinity is in the picomolar range (Choi *et al.*, 2006), suggests that if cadherin phosphorylation is regulated in cells, it would have profound consequences for catenin-binding and adhesive functions.

The kinase(s) that phosphorylate the cadherin and signals that regulate this phosphorylation are not known. Pharmacologic inhibitors, kinase-null MEFs, and dominant-negative versions of kinases known to phosphorylate the cadherin in vitro (e.g., GSK3, CK2) fail to inhibit formation of the slower-migrating, phospho form of the cadherin cytodomain (Supplemental Figure S6). These findings suggest either that these kinases are not the in vivo cadherin kinase or that cadherin phosphorylation is complex and mediated by multiple kinases.

Evidence that serines 840, 846, and 847 of E-cadherin are responsible for most radioactive phosphate incorporation is consistent with their being major phosphorylation sites. However, it is also possible that these sites are required for kinase recognition or priming and that phosphorylation occurs at other serines within the β-catenin–binding domain. Therefore definitive evidence that serines 840, 846, and 847 are phosphorylated will require confirmation using phosphoproteomics approaches, which are currently underway. Nonetheless, evidence that negative charge substitution at serines 840, 846, and 847 mimics the wild-type cadherin in most assays (i.e., steady-state endocytosis, adhesion, and motility) certainly suggests that the cadherin is modified by phosphorylation at these sites. Moreover, our inability to find cellular contexts in which the phosphomimic and WT cadherin significantly differ suggests that cadherin phosphorylation is largely constitutive under the limited set of cell culture conditions examined.

Although future studies will be required to understand the signals and machinery that regulate cadherin phosphorylation, our analysis of phosphomutant (3S>A) and phosphomimic (3S>D) cadherins provides a framework for expectations. For example, evidence that the 3S>A mutant shows reduced β-catenin binding and cell surface stability raises the question of whether inhibition of cadherin phosphorylation, and thereby reduced β-catenin binding, could promote rapid removal of E-cadherin from the cell surface. In this regard, an EMT in sea urchin known as primary mesenchymal cell ingression manifests rapid cadherin endocytosis and turnover (within 30 min) through a mechanism that is clearly independent of cadherin gene repression (Wu *et al.*, 2007; Wu and McClay, 2007). Whether cadherin phosphorylation might be inhibited during early stages of EMT to promote bulk cadherin surface removal might be worth consideration.

Whereas p120^{ctn} is generally viewed as the master regulator of cadherin surface stability (Kowalczyk and Reynolds, 2004), our findings are a reminder that β-catenin binding is also critical to cadherin surface stability. E-cadherin binds to β-catenin soon after its synthesis in the endoplasmic reticulum, and the two proteins traffic together to the basolateral membrane (Hinck *et al.*, 1994a; Chen *et al.*, 1999; Miranda *et al.*, 2003). Deletion of the β-catenin–binding domain can lead to E-cadherin accumulation within the *trans*-Golgi network, early endosomes, and lysosomes (Miyashita and Ozawa, 2007), similar to the E-cadherin trafficking defects seen in β-catenin/plakoglobin double-null F9 cells (Fukunaga *et al.*, 2005). Recent work shows that p120^{ctn} binding to cadherins obscures an acidic residue–rich endocytosis motif (Nanes *et al.*, 2012). Similarly, β-catenin binding obscures a PEST-rich protein degradation motif in E-cadherin (Huber *et al.*, 2001) and may allosterically obscure the dileucine motif that is membrane proximal to the β-catenin–binding domain, thereby preventing E-cadherin targeting to the lysosome (Miyashita and Ozawa, 2007). The role of β-catenin in cadherin stability has been overshadowed by p120^{ctn}, perhaps because there are few examples of signals that strongly affect the β-catenin/cadherin binding interaction. Moreover, modifications that affect β-catenin/cadherin binding more modestly, such as phosphorylation of β-catenin at tyrosine 654 (Roura *et al.*, 1999), clearly affect cadherin function without obviously affecting cadherin surface levels (van Veelen *et al.*, 2011; Tamada *et al.*, 2012). Understanding the conditions in which cadherin phosphorylation is

inhibited and the consequences of that inhibition for cadherin turnover is required to understand the relative contributions of p120^{ctn} and β-catenin to cadherin trafficking and stability.

MATERIALS AND METHODS

DNA constructs

Constructs used. The full-length human E-cadherin pcDNA3 and IL-2R human E-cadherin cytoplasmic domain fusion plasmids were described in Gottardi *et al*. (2001), the pCS2+6x myc-tag (MT) containing the *Xenopus* C-cadherin cytoplasmic domain was described in Fagotto *et al*. (1996), and the E-cadherin Dendra2 C-terminal fusion was described in Hong *et al*. (2010).

Constructs generated. Myr-myc-E-cad cyto/Myr*-myc-E-cad cyto: Wild-type (myr) or a point mutant (myr*) v-Src myristoylation sequence (Aronheim *et al*., 1994) was amplified from the mammalian expression vector pRSV.HB using the primers 5′-CGGGATCCCGGACCATGGGGAGTAGCAAG-3′ (forward) and 5′-CCATCGATGGCAAGATCTCCCGGGCCG-3′ (reverse) and subcloned into pCS2+6MT upstream of the 6-myc tags using *Bam*HI and *Cla*I restriction sites. E-cadherin cytoplasmic domain was PCR amplified from pCDNA3.1/E-cadherin (Gottardi *et al*., 2001) using primers 5′-GGAATTCCCGGAGGAGAGCGGTCC-3′ (forward) and 5′-GCTCTAGAGCTAGTCGTCCTCGCCGC-3′ (reverse) and subcloned into the myr or myr* pCS2+6MT vector with *Eco*RI and *Xba*I restriction sites.

Site-directed mutagenesis. All site-directed mutagenesis was carried out using the QuikChange Mutagenesis Kit (Stratagene, Agilent Technologies, Santa Clara, CA). Primers are available upon request.

Cell culture

HEK293T, MDCK, and COS-7 cells were obtained from the American Type Culture Collection. A431D cells were provided by Sergey Troyanovsky (Northwestern University, Chicago, IL). All cell types listed were maintained in DMEM (Corning, New York, NY) containing 10% fetal bovine serum (FBS; Atlanta Biologicals or JRS Scientific, Woodland, CA), 100 U/ml penicillin, and 100 μg/ml streptomycin (Corning). To generate the myr-E-cad cyto HEK293T stable line, cells were transfected with the myristoylated human E-cadherin cytoplasmic domain plasmid and the hygromycin resistance vector pCB7 (Michael Roth, UT Southwestern, Dallas, TX) in a 1:10 ratio using Lipofectamine 2000 (Invitrogen, Carlsbad, CA). Cells were selected with 0.25 mg/ml hygromycin B (Calbiochem), and drug-resistant colonies were pooled. To generate E-cadherin-Dendra2 lines, cells were transfected with E-cadherin-Dendra2 using Effectene (Qiagen, Hilden, Germany) and selected with 800 μg/ml G418 (Corning). Resistant colonies were pooled and sorted for Dendra2 fluorescence by flow cytometry using a MoFlo Legacy (BD Biosciences) or FacsAria5 (BD Biosciences, San Jose, CA). IL2R-E-cadherin lines were generated by transfection of IL2R-E-cadherin with the G418 resistance vector pcDNA3 in a ratio of 1:10 using Effectene, selection with 800 μg/ml G418, and pooling of resistant colonies.

Antibodies

We used mouse monoclonal anti–β-catenin clone 14 (BD Transduction Laboratories), rabbit polyclonal anti–β-catenin (06-734; Millipore), mouse monoclonal anti–E-cadherin HECD-1 (Zymed, San Francisco, CA), rabbit polyclonal anti–α-catenin clone H-297 (Santa Cruz Biotechnology, Santa Cruz, CA), mouse monoclonal anti–β-tubulin Tub2.1 (Sigma-Aldrich, St. Louis, MO), rabbit polyclonal anti-Dendra2 (ABIN361314; antibodies-online), rabbit polyclonal anti–glyceraldehyde-3-phosphate dehydrogenase FL-335 (Santa Cruz Biotechnology), mouse monoclonal anti-Lamp2 9A182 (US Biological), mouse monoclonal anti-GM130 35 (BD Transduction Laboratories), mouse monoclonal anti–ZO-1 1A12 (Invitrogen), mouse monoclonal anti–IL-2R alpha 24212 (R&D Systems, Minneapolis, MN), mouse monoclonal anti–Na^+/K^+ ATPase α-1 C464.6 (Millipore, Temecula, CA), rabbit polyclonal anti-LRP6 C5C7 (Cell Signaling, Beverly, MA), mouse monoclonal anti-myc 9E10 (Sigma-Aldrich), goat anti-mouse and goat anti-rabbit IRDye680RD and IRDye800CW (Li-Cor Biosciences, Lincoln, NE), goat anti-mouse and goat anti-rabbit horseradish peroxidase (Bio-Rad, Hercules, CA), and goat anti-mouse and goat anti-rabbit Alexa 488 and Alexa 568 (Invitrogen).

Affinity precipitation and Western blotting

Cells were lysed in buffer containing 50 mM Tris, pH 7.5, 5 mM EDTA, 150 mM NaCl, 5% glycerol, and 1% Triton X-100 with protease inhibitor cocktail (Roche, Nutley, NJ). For immunoprecipitations, lysates were incubated with indicated antibodies and ImmunoPure Immobilized Protein G or Protein A (Pierce, Rockford, IL). Precipitated proteins were washed and subjected to SDS–PAGE and Western blot analysis using standard procedures. Blots were imaged with either standard dark room procedures using film and ECL (Amersham, Pittsburgh, PA) or digitally using a Li-Cor Odyssey blot imager (Li-Cor Biosciences). Densitometry was carried out using ImageJ (National Institutes of Health, Bethesda, MD) or Li-Cor Image Studio software.

[^{35}S]methionine/cysteine metabolic labeling

Steady-state metabolic labeling of proteins with [^{35}S]methionine/cysteine was performed as previously described (Gottardi and Gumbiner, 2004). Briefly, cells were labeled overnight with 1–2 mCi/10-cm dish Redivue PRO-MIX [^{35}S] cell labeling mix (Amersham). Pulse-chase [^{35}S]methionine/cysteine metabolic labeling was performed as described previously (Gottardi and Caplan, 1993; Hinck *et al*., 1994b). Cells were incubated in methionine/cysteine-free DMEM (Sigma-Aldrich) for 30 min at 37°C to deplete intracellular pools and then pulsed with 200 μCi of EasyTag EXPRESS [^{35}S]-Protein Labeling Mix (PerkinElmer, Naperville, IL) for 20 min at 37°C. Cells were chased with DMEM containing excess unlabeled L-methionine or L-cysteine (0.3 mg/ml; Sigma-Aldrich) at 37°C for the times indicated. Cells were lysed in 1% Triton buffer described earlier before immunoprecipitation with anti-myc antibody.

[^{32}P]orthophosphate labeling

We transiently transfected 1×10^6 COS-7 cells in suspension with Lipofectamine 2000 (Invitrogen). After 36 h, cells were washed twice in phosphate-buffered saline (PBS) and incubated in phosphate-free labeling media for 30 min. Cells were labeled for 3 h with 120 μCi of [^{32}P]orthophosphate (PerkinElmer) in labeling medium before lysis. Immunoprecipitated proteins were separated on 10% SDS–PAGE gels and subjected to autoradiography. Western blot analysis was performed on a portion of each sample to confirm efficiency of immunoprecipitation.

Phosphatase experiment

Immunoprecipitated complexes were treated with λ protein phosphatase (New England BioLabs, Ipswich, MA) according to the manufacturer's instructions. Samples were also incubated with phosphatase inhibitors (10 mM sodium vanadate [tyrosine; Sigma-Aldrich] and 50 mM sodium fluoride [serine/threonine; Sigma-Aldrich]) as indicated. Reaction was performed at 30°C for 30 min

and quenched with Laemmli sample buffer before Western blot analysis.

Monolayer dispersion assay

Cells were plated in 12-well cell culture dishes at a seeding density of 0.5×10^6 cells. After 48 h, the cells were rinsed in PBS supplemented with Ca^{2+} and Mg^{2+} (1 and 0.5 mM, respectively) and then incubated in 1 mg/ml dispase (Roche) enzyme in Hank's balanced salt solution (Corning) supplemented with 1.2 mM Ca^{2+}. After being lifted from the dish, cell monolayers were subjected to a shaking force of 1400 rpm. After 10 min of shaking, macroscopic fragments were counted with a dissecting microscope. If no macroscopic fragments were present, microscopic fragments were counted with a hemocytometer.

Inhibition of lysosomal degradation

Cells were treated with 200 µM chloroquine diphosphate or an equivalent volume of PBS for 24 h.

Fluorescence-based endocytosis assay

A fluorescence-based assay to follow the endocytosis of IL2R-E-cadherin chimeras was carried out as described in Nanes *et al.* (2012). Cells were switched into calcium-free DMEM (Life Technologies, Grand Island, NY) with 10% dialyzed FBS (Life Technologies) 24 h before labeling. Cells were labeled with anti–IL-2R in calcium-free culture medium at 4°C for 30 min. After unbound antibody was removed with a brief wash in PBS, cells were incubated in culture medium at 37°C for 10 min to induce endocytosis. Cells were subsequently returned to 4°C and rinsed, and the remaining surface antibody was stripped with a low-pH wash (PBS with 100 mM glycine, 20 mM magnesium acetate, and 50 mM potassium chloride, pH 2.2). One sample was not returned to 37°C nor subjected to an acid wash and served as a control for labeling efficiency. An additional sample was not returned to 37°C but was subjected to an acid wash and served as a control for antibody-stripping efficiency. Cells were then rinsed and processed for immunofluorescence. Internalization was quantified by measuring the fluorescence intensity after 10 min and normalizing to fluorescence intensity preendocytosis (labeling efficiency control). All measurements were made using ImageJ.

Cell surface biotinylation

Surface biotinylation was performed as described elsewhere (Gottardi *et al.*, 1995). In brief, cells were rinsed in PBS without calcium or magnesium (PBS^-) and labeled at 4°C for 30 min with 0.5 mg/ml sulfo-NHS-SS biotin (Pierce) in PBS^-. The reaction was quenched with 20 mM glycine in PBS^-. To assess the degradation kinetics of biotinylatable (surface) proteins, cells were placed at 37°C to induce endocytosis (and subsequent degradation) for various time points, washed with PBS^-, and lysed with 1% Triton buffer described earlier. Biotinylated proteins were then enriched by affinity purification with NeutrAvidin beads (Pierce). To assess endocytosis rates, labeled cells were returned to 37°C for various time points but were then placed back on ice. Remaining biotin on the cell surface was stripped with MesNA (Sigma-Aldrich) in 50 mM Tris, pH 8.6, 100 mM NaCl, and 2.5 mM $CaCl_2$ followed by an alkylation step with 5 mg/ml iodoacetamide (Bio-Rad) in PBS^-. Cells were washed with PBS^- before lysis and enrichment as described. One plate for each condition was not placed at 37°C and served as a control for total labeling efficiency, and an additional plate was not placed at 37°C but was subjected to the stripping and alkylation steps as a control for stripping efficiency.

Immunofluorescence

Cells were plated on glass coverslips treated overnight with 1 µg/ml bovine fibronectin (Millipore) for A431D cells or 0.1% porcine gelatin (Sigma-Aldrich) for MDCK cells. Cells were fixed in ice-cold anhydrous methanol and processed using standard procedures. Coverslips were mounted with Aqua Poly/Mount (Polysciences, Warrington, PA) or Prolong Gold (Invitrogen). Images to quantify internalization were captured with the Axioplan 2 microscope (Zeiss, Thornwood, NY) equipped with a 40× Plan-Neofluar, numerical aperture (NA) 0.75 objective and AxioCam HRm camera using AxioVision4.8 software (Zeiss). All other images are confocal and were captured using a Nikon A1R microscope equipped with a 60× Plan Apo, NA 1.45 objective and resonant scanner using Nikon Elements Software. Colocalization analysis was carried out on *z*-stacks using ImageJ software.

Statistics

Statistics were computed using Prism (GraphPad, La Jolla, CA). Analysis of variance (ANOVA) between groups with Tukey's multiple comparison test was used to evaluate data.

ACKNOWLEDGMENTS

We thank Benjamin Nanes and Andrew Kowalczyk for advice on the IL-2R–based endocytosis assay and members of the Gottardi lab for critically reading the manuscript. Cell sorting was performed at the Northwestern University Flow Cytometry Facility, which is supported by a Cancer Center Support Grant (National Cancer Institute CA060553). Imaging work was performed at the Northwestern University Cell Imaging Facility, which is supported by National Cancer Institute CCSG P30 CA060553 awarded to the Robert H. Lurie Comprehensive Cancer Center. A.E.M. is supported in part by the Malkin Scholars Program from the Robert H. Lurie Comprehensive Cancer Center of Northwestern University, National Institutes of Health/National Heart, Lung, and Blood Institute T32HL076139 Training Grant, and National Institutes of Health/National Cancer Institute F30 CA171944-01A1. C.J.G. is supported by National Institutes of Health GM076561 and HL094643.

REFERENCES

Aronheim A, Engelberg D, Li N, al-Alawi N, Schlessinger J, Karin M (1994). Membrane targeting of the nucleotide exchange factor Sos is sufficient for activating the Ras signaling pathway. Cell 78, 949–961.

Bullions LC, Notterman DA, Chung LS, Levine AJ (1997). Expression of wild-type alpha-catenin protein in cells with a mutant alpha-catenin gene restores both growth regulation and tumor suppressor activities. Mol Cell Biol 17, 4501–4508.

Chen YT, Stewart DB, Nelson WJ (1999). Coupling assembly of the E-cadherin/beta-catenin complex to efficient endoplasmic reticulum exit and basal-lateral membrane targeting of E-cadherin in polarized MDCK cells. J Cell Biol 144, 687–699.

Choi HJ, Huber AH, Weis WI (2006). Thermodynamics of beta-catenin-ligand interactions: the roles of the N- and C-terminal tails in modulating binding affinity. J Biol Chem 281, 1027–1038.

Dukes JD, Whitley P, Chalmers AD (2011). The MDCK variety pack: choosing the right strain. BMC Cell Biol 12, 43.

Fagotto F, Funayama N, Gluck U, Gumbiner BM (1996). Binding to cadherins antagonizes the signaling activity of beta-catenin during axis formation in *Xenopus*. J Cell Biol 132, 1105–1114.

Fukunaga Y, Liu H, Shimizu M, Komiya S, Kawasuji M, Nagafuchi A (2005). Defining the roles of beta-catenin and plakoglobin in cell-cell adhesion: isolation of beta-catenin/plakoglobin-deficient F9 cells. Cell Struct Funct 30, 25–34.

Gottardi CJ, Caplan MJ (1993). Delivery of Na+,K(+)-ATPase in polarized epithelial cells. Science 260, 552–556.

Gottardi CJ, Dunbar LA, Caplan MJ (1995). Biotinylation and assessment of membrane polarity: caveats and methodological concerns. Am J Physiol 268, F285–F295.

Gottardi CJ, Gumbiner BM (2004). Distinct molecular forms of beta-catenin are targeted to adhesive or transcriptional complexes. J Cell Biol 167, 339–349.
Gottardi CJ, Wong E, Gumbiner BM (2001). E-cadherin suppresses cellular transformation by inhibiting beta-catenin signaling in an adhesion-independent manner. J Cell Biol 153, 1049–1060.
Gumbiner B, Simons K (1987). The role of uvomorulin in the formation of epithelial occluding junctions. CIBA Found Symp 125, 168–186.
Hinck L, Nathke IS, Papkoff J, Nelson WJ (1994a). Dynamics of cadherin/catenin complex formation: novel protein interactions and pathways of complex assembly. J Cell Biol 125, 1327–1340.
Hinck L, Nelson WJ, Papkoff J (1994b). Wnt-1 modulates cell-cell adhesion in mammalian cells by stabilizing beta-catenin binding to the cell adhesion protein cadherin. J Cell Biol 124, 729–741.
Hong S, Troyanovsky RB, Troyanovsky SM (2010).Spontaneous assembly and active disassembly balance adherens junction homeostasis. Proc Natl Acad Sci USA 107, 3528–3533.
Huber AH, Stewart DB, Laurents DV, Nelson WJ, Weis WI (2001). The cadherin cytoplasmic domain is unstructured in the absence of beta-catenin. A possible mechanism for regulating cadherin turnover. J Biol Chem 276, 12301–12309.
Huber AH, Weis WI (2001). The structure of the beta-catenin/E-cadherin complex and the molecular basis of diverse ligand recognition by beta-catenin. Cell 105, 391–402.
Kowalczyk AP, Nanes BA (2012). Adherens junction turnover: regulating adhesion through cadherin endocytosis, degradation, and recycling. Subcell Biochem 60, 197–222.
Kowalczyk AP, Reynolds AB (2004). Protecting your tail: regulation of cadherin degradation by p120-catenin. Curr Opin Cell Biol 16, 522–527.
Larue L, Ohsugi M, Hirchenhain J, Kemler R (1994). E-cadherin null mutant embryos fail to form a trophectoderm epithelium. Proc Natl Acad Sci USA 91, 8263–8267.
Le TL, Yap AS, Stow JL (1999). Recycling of E-cadherin: a potential mechanism for regulating cadherin dynamics. J Cell Biol 146, 219–232.
Lee E, Salic A, Kruger R, Heinrich R, Kirschner MW (2003). The roles of APC and Axin derived from experimental and theoretical analysis of the Wnt pathway. PLoS Biol 1, E10.
Lewis JE, Wahl JK 3rd, Sass KM, Jensen PJ, Johnson KR, Wheelock MJ (1997). Cross-talk between adherens junctions and desmosomes depends on plakoglobin. J Cell Biol 136, 919–934.
Lickert H, Bauer A, Kemler R, Stappert J (2000). Casein kinase II phosphorylation of E-cadherin increases E-cadherin/beta-catenin interaction and strengthens cell-cell adhesion. J Biol Chem 275, 5090–5095.
Maiden SL, Harrison N, Keegan J, Cain B, Lynch AM, Pettitt J, Hardin J (2013). Specific conserved C-terminal amino acids of *Caenorhabditis elegans* HMP-1/alpha-catenin modulate F-actin binding independently of vinculin. J Biol Chem 288, 5694–5706.
McEwen AE, Escobar DE, Gottardi CJ (2012). Signaling from the adherens junction. Subcell Biochem 60, 171–196.
Miranda KC, Joseph SR, Yap AS, Teasdale RD, Stow JL (2003). Contextual binding of p120ctn to E-cadherin at the basolateral plasma membrane in polarized epithelia. J Biol Chem 278, 43480–43488.
Miyashita Y, Ozawa M (2007). A dileucine motif in its cytoplasmic domain directs beta-catenin-uncoupled E-cadherin to the lysosome. J Cell Sci 120, 4395–4406.
Nanes BA, Chiasson-MacKenzie C, Lowery AM, Ishiyama N, Faundez V, Ikura M, Vincent PA, Kowalczyk AP (2012). p120-catenin binding masks an endocytic signal conserved in classical cadherins. J Cell Biol 199, 365–380.
Nelson WJ (2008). Regulation of cell-cell adhesion by the cadherin-catenin complex. Biochem Soc Trans 36, 149–155.
Niessen CM, Leckband D, Yap AS (2011). Tissue organization by cadherin adhesion molecules: dynamic molecular and cellular mechanisms of morphogenetic regulation. Physiol Rev 91, 691–731.
Ozawa M, Ringwald M, Kemler R (1990). Uvomorulin-catenin complex formation is regulated by a specific domain in the cytoplasmic region of the cell adhesion molecule. Proc Natl Acad Sci USA 87, 4246–4250.
Peifer M, Orsulic S, Sweeton D, Wieschaus E (1993). A role for the *Drosophila* segment polarity gene armadillo in cell adhesion and cytoskeletal integrity during oogenesis. Development 118, 1191–1207.
Petrova YI, Spano MM, Gumbiner BM (2012). Conformational epitopes at cadherin calcium-binding sites and p120-catenin phosphorylation regulate cell adhesion. Mol Biol Cell 23, 2092–2108.
Posthaus H, Dubois CM, Laprise MH, Grondin F, Suter MM, Muller E (1998). Proprotein cleavage of E-cadherin by furin in baculovirus over-expression system: potential role of other convertases in mammalian cells. FEBS Lett 438, 306–310.
Roura S, Miravet S, Piedra J, Garcia de Herreros A, Dunach M (1999). Regulation of E-cadherin/catenin association by tyrosine phosphorylation. J Biol Chem 274, 36734–36740.
Sarpal R, Pellikka M, Patel RR, Hui FY, Godt D, Tepass U (2012). Mutational analysis supports a core role for *Drosophila* alpha-catenin in adherens junction function. J Cell Sci 125, 233–245.
Sefton M, Johnson MH, Clayton L (1992). Synthesis and phosphorylation of uvomorulin during mouse early development. Development 115, 313–318.
Serres M, Filhol O, Lickert H, Grangeasse C, Chambaz EM, Stappert J, Vincent C, Schmitt D (2000). The disruption of adherens junctions is associated with a decrease of E-cadherin phosphorylation by protein kinase CK2. Exp Cell Res 257, 255–264.
Simcha I, Kirkpatrick C, Sadot E, Shtutman M, Polevoy G, Geiger B, Peifer M, Ben-Ze'ev A (2001). Cadherin sequences that inhibit beta-catenin signaling: a study in yeast and mammalian cells. Mol Biol Cell 12, 1177–1188.
Stappert J, Kemler R (1994). A short core region of E-cadherin is essential for catenin binding and is highly phosphorylated. Cell Adhes Commun 2, 319–327.
Tamada M, Farrell DL, Zallen JA (2012). Abl regulates planar polarized junctional dynamics through beta-catenin tyrosine phosphorylation. Dev Cell 22, 309–319.
Tan CW, Gardiner BS, Hirokawa Y, Layton MJ, Smith DW, Burgess AW (2012). Wnt signalling pathway parameters for mammalian cells. PloS One 7, e31882.
Tepass U, Gruszynski-DeFeo E, Haag TA, Omatyar L, Torok T, Hartenstein V (1996). shotgun encodes *Drosophila* E-cadherin and is preferentially required during cell rearrangement in the neurectoderm and other morphogenetically active epithelia. Genes Dev 10, 672–685.
Torres M, Stoykova A, Huber O, Chowdhury K, Bonaldo P, Mansouri A, Butz S, Kemler R, Gruss P (1997). An alpha-E-catenin gene trap mutation defines its function in preimplantation development. Proc Natl Acad Sci USA 94, 901–906.
Tunggal JA, Helfrich I, Schmitz A, Schwarz H, Gunzel D, Fromm M, Kemler R, Krieg T, Niessen CM (2005). E-cadherin is essential for in vivo epidermal barrier function by regulating tight junctions. EMBO J 24, 1146–1156.
van Veelen W *et al*. (2011). beta-Catenin tyrosine 654 phosphorylation increases Wnt signalling and intestinal tumorigenesis. Gut 60, 1204–1212.
Vasioukhin V, Bauer C, Degenstein L, Wise B, Fuchs E (2001). Hyperproliferation and defects in epithelial polarity upon conditional ablation of alpha-catenin in skin. Cell 104, 605–617.
Wodarz A, Stewart DB, Nelson WJ, Nusse R (2006). Wingless signaling modulates cadherin-mediated cell adhesion in *Drosophila* imaginal disc cells. J Cell Sci 119, 2425–2434.
Wu SY, Ferkowicz M, McClay DR (2007). Ingression of primary mesenchyme cells of the sea urchin embryo: a precisely timed epithelial mesenchymal transition. Birth Defects Res C Embryo Today 81, 241–252.
Wu SY, McClay DR (2007). The Snail repressor is required for PMC ingression in the sea urchin embryo. Development 134, 1061–1070.
Xiao K, Garner J, Buckley KM, Vincent PA, Chiasson CM, Dejana E, Faundez V, Kowalczyk AP (2005). p120-Catenin regulates clathrin-dependent endocytosis of VE-cadherin. Mol Biol Cell 16, 5141–5151.
Yap AS, Brieher WM, Pruschy M, Gumbiner BM (1997). Lateral clustering of the adhesive ectodomain: a fundamental determinant of cadherin function. Curr Biol 7, 308–315.